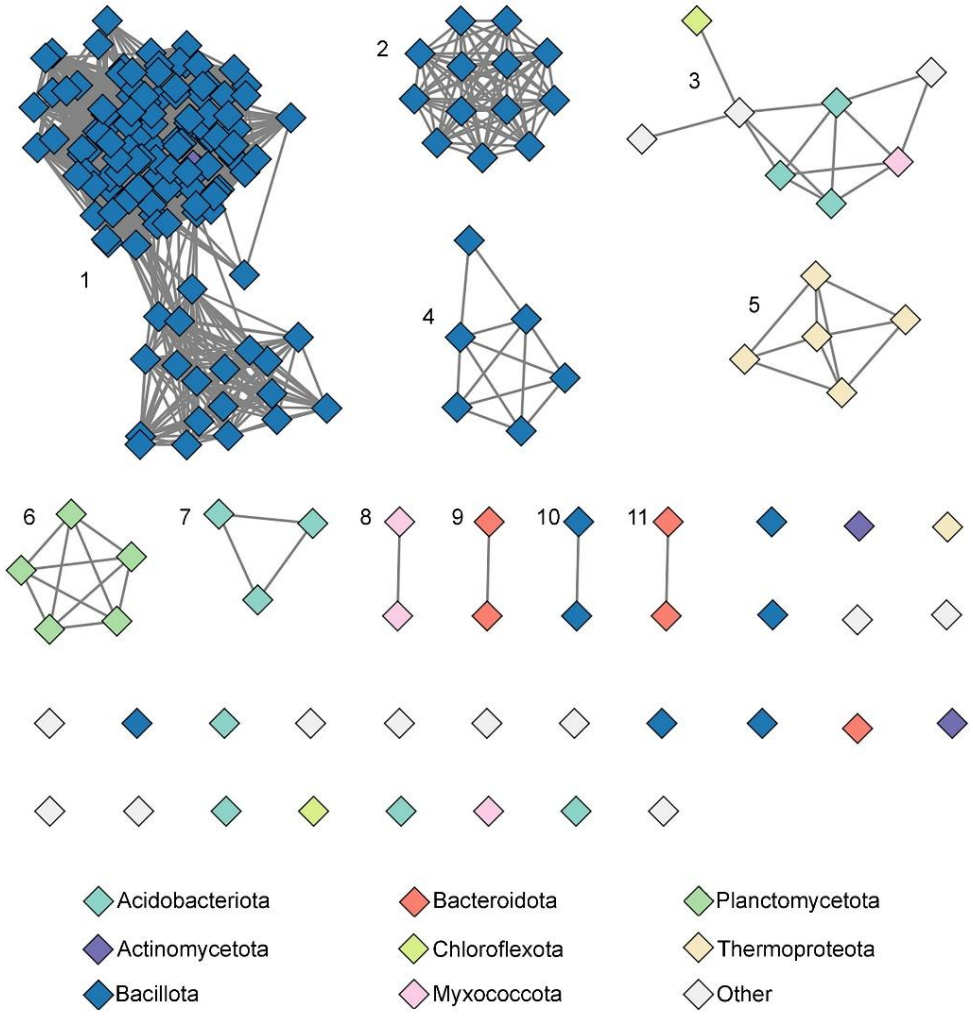

Supplementary Figure 1. Sequence similarity network of proteins, homologous to the signal peptidase I from the *lpp* biosynthetic gene cluster of *Paenibacillus alginolyticus* DSM5050 (WP_029196374.1). Edges corresponding to an E-value higher than 10e-23 are removed. Nodes are colored according to the phylum.

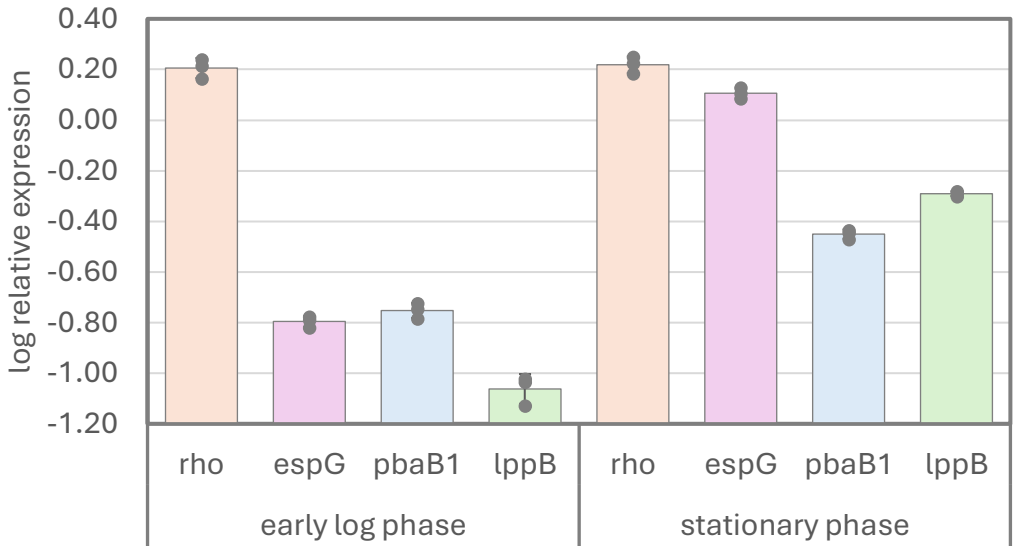

Supplementary Figure 2. RT-qPCR analysis of *lpp* and *pba* BGCs expression levels in *Paenibacillus alginolyticus* DSM5050 cells harvested at early logarithmic and stationary growth phases in 1/2 LB medium. Data were normalized to the expression level of the constitutively expressed *gyrA*. Expression of *rho* was used as a positive technical control. *espG* (PAL01S_RS16325) is the exopolysaccharide chain length-determining protein tyrosine kinase gene colocalized with *lpp* and *pba* (Supplementary Figure 3). Data from 3 individual replicates are shown as dots. Source data are provided as a Source Data file.

A

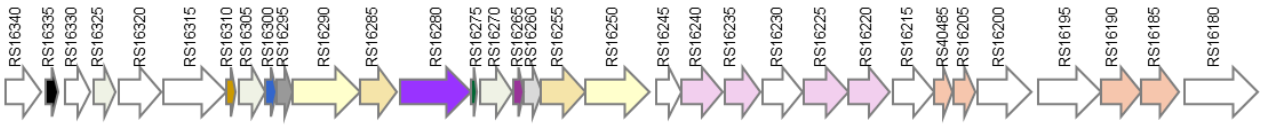

B

Locus tag	Protein family	Annotation	Name
PAL01S_RS16340	TIGR00277	HDIG: HDIG domain	
PAL01S_RS16335	TIGR03020	EpsA: transcriptional regulator EpsA	
PAL01S_RS16330	TIGR01006	polys_exp_MPA1: polysaccharide export protein, MPA1 family	
PAL01S_RS16325	TIGR03029	EpsG: chain length determinant protein tyrosine kinase EpsG	
PAL01S_RS16320	TIGR01730	RND_mfp: efflux transporter, RND family, MFP subunit	
PAL01S_RS16310	No match		
PAL01S_RS16315	No match		*lppA*^{LC}
PAL01S_RS16305	TIGR04352	HprK_rel_A: HprK-related kinase A	*lppK*
PAL01S_RS16300	RREFam002	Discrete RRE protein in a lasso peptide cluster	*lppB*
PAL01S_RS16295	TIGR02228	sigpep_I_arch: signal peptidase I	*lppS*
PAL01S_RS16290	TIGR02204	MsbA_rel: ABC transporter, permease/ATP-binding protein	*lppD*
PAL01S_RS16285	PF14907	Uncharacterized nucleotidyltransferase	*lppN*
PAL01S_RS16280	TIGR01536	asn_synth_AEB: asparagine synthase (glutamine-hydrolyzing)	*pbaC*
PAL01S_RS16275	No match		*pbaA*^{LC}
PAL01S_RS16270	TIGR04352	HprK_rel_A: HprK-related kinase A	*pbaK*
PAL01S_RS16265	RREFam002	Discrete RRE protein in a lasso peptide cluster	*pbaB1*
PAL01S_RS16260	PF13471	Transglutaminase-like superfamily	*pbaB2*
PAL01S_RS16255	PF14907	Uncharacterized nucleotidyltransferase	*pbaN*
PAL01S_RS16250	TIGR02203	MsbA_lipidA: lipid A export permease/ATP-binding protein MsbA	*pbaD*
PAL01S_RS16245	PF05704	Capsular polysaccharide synthesis protein	
PAL01S_RS16240	PF00534	Glycosyl transferases group 1	
PAL01S_RS16235	PF00535	Glycosyl transferase family 2	
PAL01S_RS16230	PF04230	Polysaccharide pyruvyl transferase	
PAL01S_RS16225	PF00534	Glycosyl transferases group 1	
PAL01S_RS16220	PF00534	Glycosyl transferases group 1	
PAL01S_RS16215	PF07470	Glycosyl Hydrolase Family 88	
PAL01S_RS40485	TIGR03570	sugar O-acyltransferase, sialic acid O-acetyltransferase, NeuD family	
PAL01S_RS16205	TIGR03570	sugar O-acyltransferase, sialic acid O-acetyltransferase, NeuD family	
PAL01S_RS16200	No match		
PAL01S_RS16195	TIGR01923	O-succinylbenzoate-CoA ligase	
PAL01S_RS16190	PF01757	Acyltransferase family	
PAL01S_RS16185	PF01757	Acyltransferase family	
PAL01S_RS16180	PF13229	Right-handed beta helix region	

Supplementary Figure 3. Schematic representation of the *P. alginolyticus lpp* locus (A) and annotations of the genes (B). Arrows indicating genes are colored according to their putative functions. Genes used for the RT-PCR assay (Figure S2) are highlighted in blue.

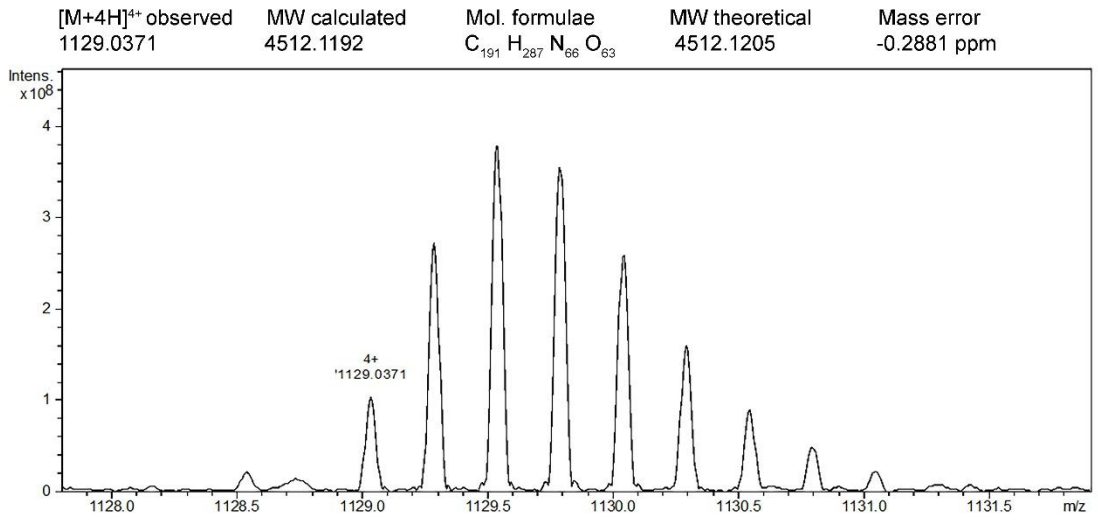

Supplementary Figure 4. High-resolution MS spectrum of the *in vivo* processed LppA^{LC}.

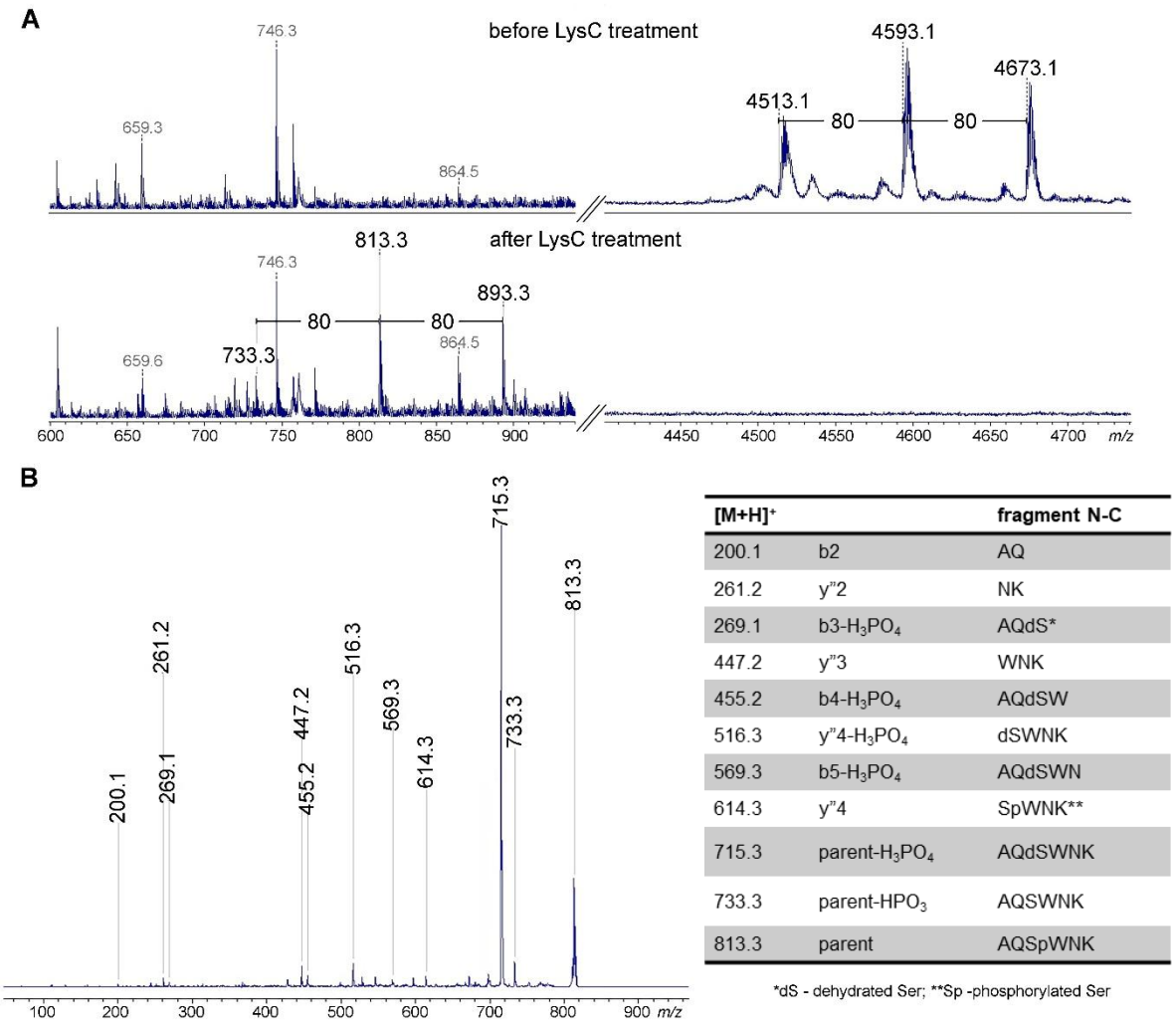

[M+H]⁺		fragment N-C
200.1	b2	AQ
261.2	y"2	NK
269.1	b3-H_3PO_4	AQdS*
447.2	y"3	WNK
455.2	b4-H_3PO_4	AQdSW
516.3	y"4-H_3PO_4	dSWNK
569.3	b5-H_3PO_4	AQdSWN
614.3	y"4	SpWNK**
715.3	parent-H_3PO_4	AQdSWNK
733.3	parent-HPO_3	AQSWNK
813.3	parent	AQSpWNK

*dS - dehydrated Ser; **Sp -phosphorylated Ser

Supplementary Figure 5. Identification of the phosphorylation site in LppA^{LC}. A. MALDI-TOF MS spectra of partially purified products of *lpp* BGC before and after treatment with LysC endoprotease recorded in reflector mode. $[M+H]^+$ mass peaks at *m/z* 4513.1, 4593.1, and 4673.1 correspond to the unphosphorylated, mono-, and di-phosphorylated LppA^C peptide. $[M+H]^+$ mass peaks at *m/z* 733.3, 813.3, and 893.3 correspond to the same peptides with the C-terminal part removed by LysC. Spectra were recorded in reflector mode with measurement accuracy within 0.1 Da. **B.** MALDI TOF MS/MS analysis of the N-terminal fragment of the monophosphorylated LppA^C peptide ($[M+H]^+$ 813.3).

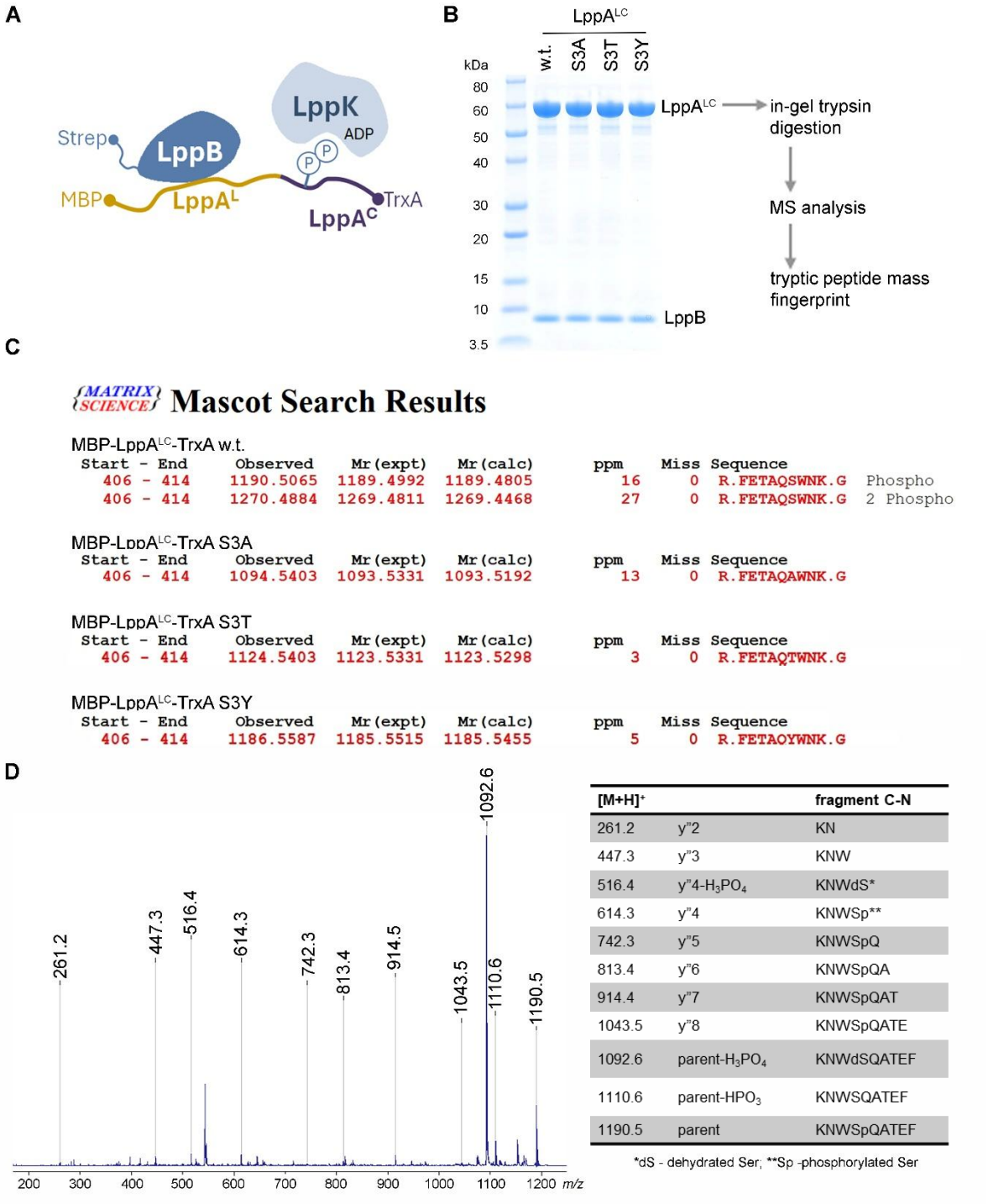

[M+H]+		fragment C-N
261.2	y"2	KN
447.3	y"3	KNW
516.4	y"4-H_3PO_4	KNWdS*
614.3	y"4	KNWSp**
742.3	y"5	KNWSpQ
813.4	y"6	KNWSpQA
914.4	y"7	KNWSpQAT
1043.5	y"8	KNWSpQATE
1092.6	parent-H_3PO_4	KNWdSQATEF
1110.6	parent-HPO_3	KNWSQATEF
1190.5	parent	KNWSpQATEF

*dS - dehydrated Ser; **Sp -phosphorylated Ser

Supplementary Figure 6. LppK kinase modifies conserved Ser3 residue in LppA^{LC}. A. Schematic representation of the assay. LppA^{LC} peptide fused with N-terminal MBP and C-terminal TrxA mass tag (MW 60.1 kDa) co-expressed with LppB harboring N-terminal Strep-tag and LppK. The LppB-LppA^{LC} complex was purified using affinity chromatography. **B.** SDS-PAGE analysis

of the eluted fractions. Mutations in $LppA^{LC}$ are shown at the top. Protein zones corresponding to $LppA^{LC}$ (MBP-$LppA^{LC}$-TrxA fused protein, MW 61.5 kDa) were subjected to in-gel digestion with trypsin. The eluted tryptic peptides were identified using MALDI-TOF MS. All pull-down experiments were performed independently three times with similar results. Source data are provided as a Source Data file. **C.** Protein modifications analysis using the Mascot protein identification tool (https://www.matrixscience.com/) with phosphorylation as a variable modification. Shown are extracts of the relevant peptide hits from the Mascot Peptide Summary. **D.** MALDI-TOF MS/MS analysis of the monophosphorylated tryptic peptide of $LppA^{LC}$ ($[M+H]^+$ 1190.5).

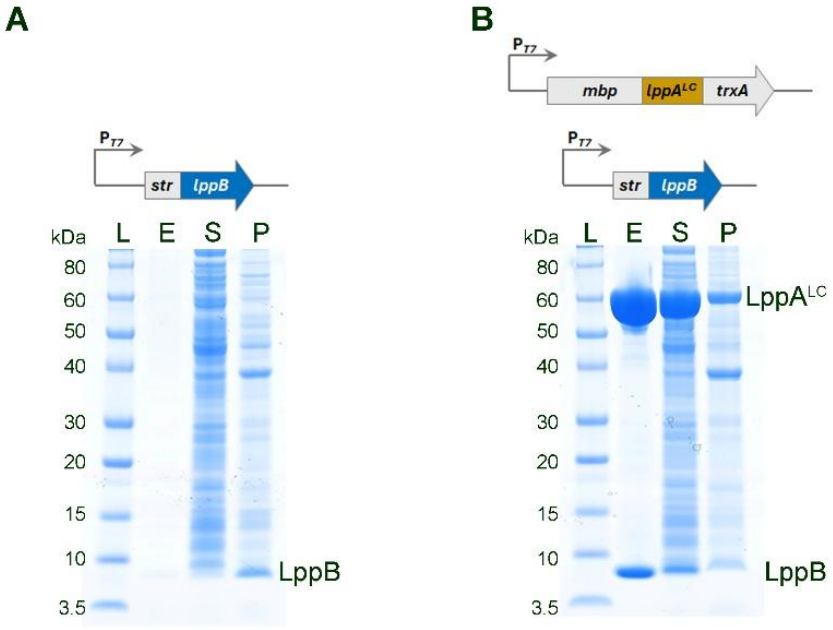

Supplementary Figure 7. Purification of LppB (A) and the LppB•LppA^{LC} complex (B). LppA^{LC} was fused to MBP and TrxA mass tags to improve resolution on PAGE; LppB was fused with Strep tag. L, protein MW molecular weight ladder; E, eluate from StrepTactin resin; S, cleared cellular lysate; P, insoluble fraction. LppA^{LC}, MBP-LppA^{LC}-TrxA fused protein, MW 61.5 kDa; LppB, Strep-tagged LppB, MW 11.1 kDa. All pull-down experiments were performed independently three times with similar results. Source data are provided as a Source Data file.

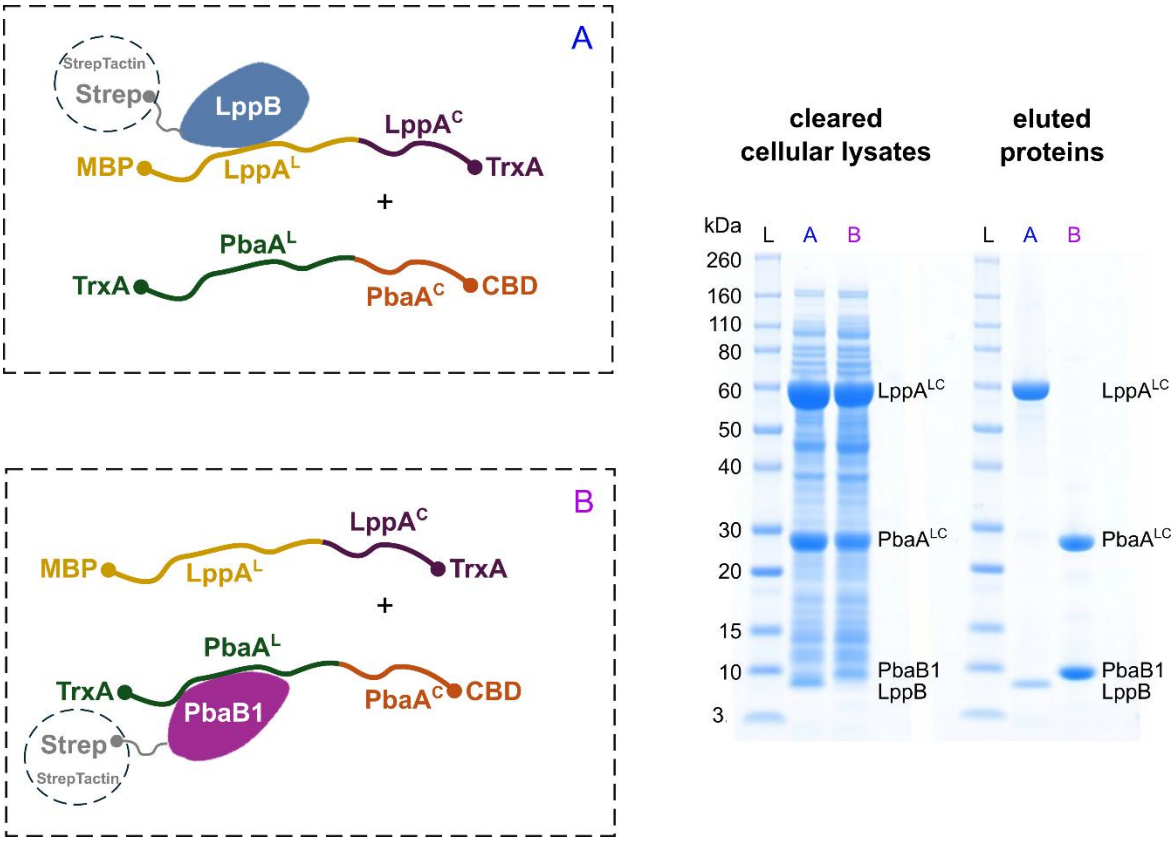

Supplementary Figure 8. Schematic representation of the competition pull-down assay (left) and cleared cellular lysates and eluted protein fractions of the competition pull-down assays of RRE-precursor peptide complexes co-expressing $LppA^{LC}$ and $PbaA^{LC}$ peptides with either Strep-tagged LppB (A) or Strep-tagged PbaB1 (B) (right). $LppA^{LC}$ was expressed as an MBP-$LppA^{LC}$-TrxA fusion (MW 61.5 kDa), and $PbaA^{LC}$ as a TrxA-$PbaA^{LC}$-CBD fusion (MW 24.6 kDa). L, protein MW ladder. All pull-down experiments were performed independently three times with similar results. Source data are provided as a Source Data file.

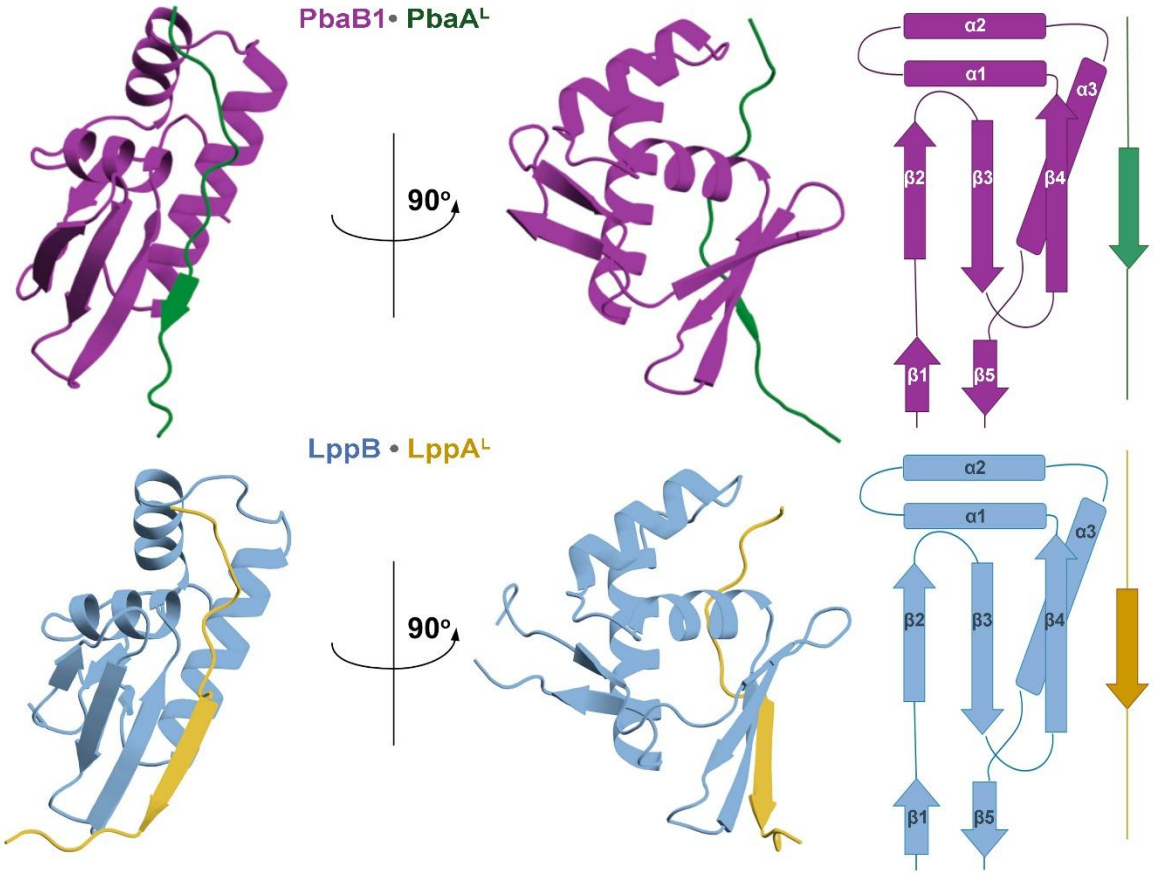

Supplementary Figure 9. Crystal structures and topology diagrams of the PbaB1•PbaA^{L} (top) and LppB•LppA^{L} (bottom) complexes. RRE proteins are shown in purple (PbaB1) or light blue (LppB), while their cognate leader peptides are depicted in green (PbaA^{L}) or yellow (LppA^{L}).

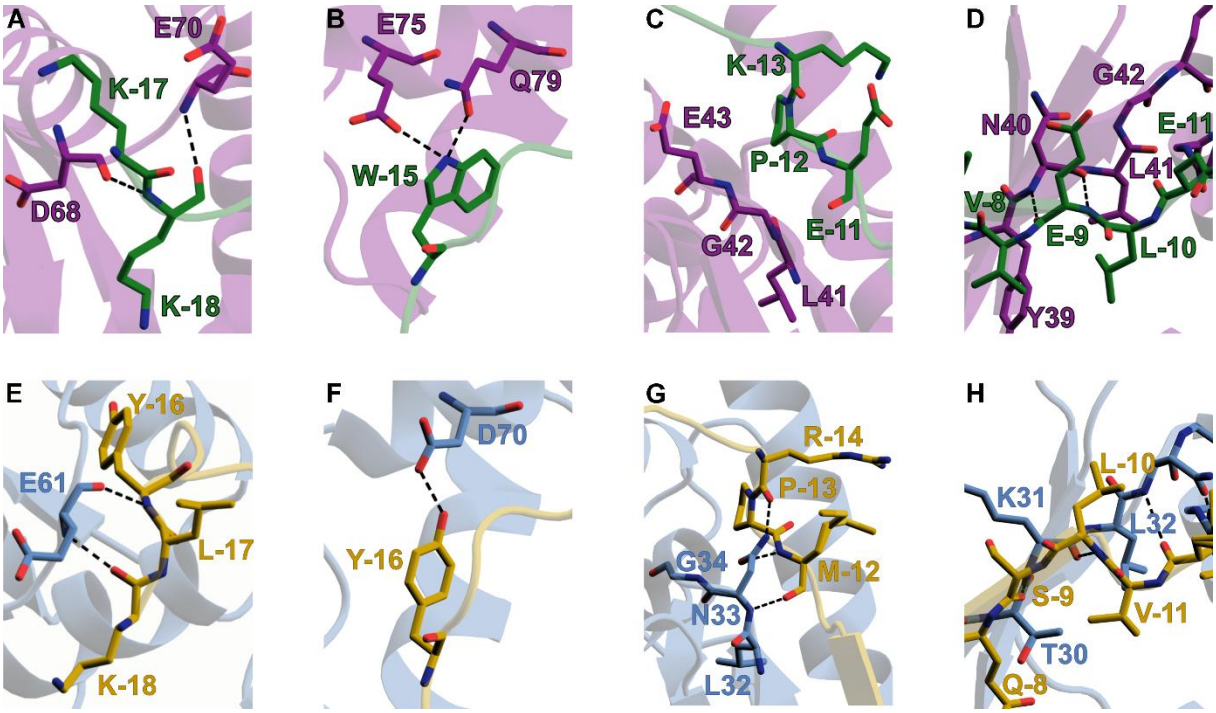

Supplementary Figure 10. Intermolecular interactions in the PbaB1•PbaA^{L} (A-D) and LppB•LppA^{L} (E-H) complexes. Residues in the PbaA^{L} and LppA^{L} leader peptides are shown in green and yellow, respectively. PbaB1 and LppB RRE domains are in magenta and blue, respectively. Hydrogen bonds are indicated with black dashed lines. Alternative conformations are shown for LppA^{L} M-12.

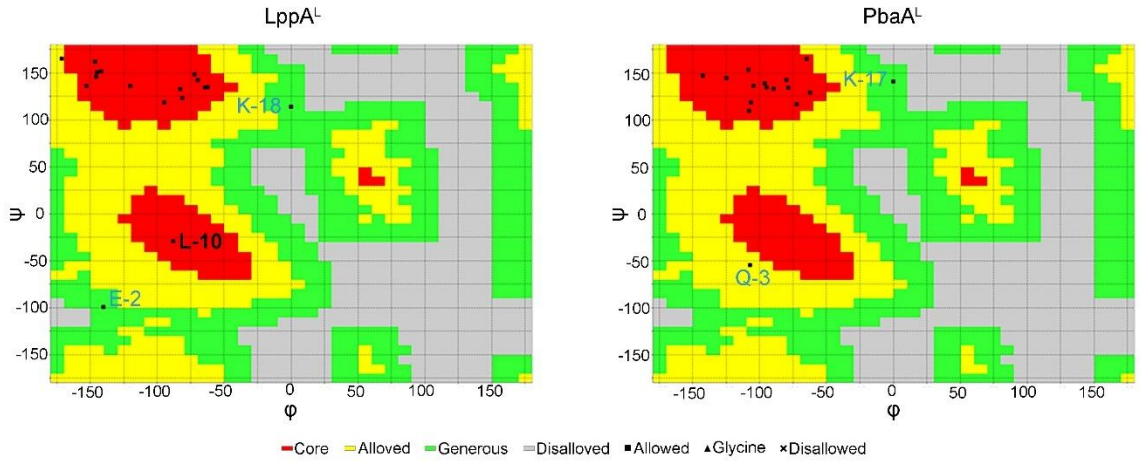

Supplementary Figure 11. Ramachandran plots of the LppA^L and PbaA^L peptides. Coordinates for the peptides were obtained from the pdb_00009x8z (LppB•LppA^L) and pdb_00009x90 (PbaB•PbaA^L) structures and analyzed using the VADAR protein structure analysis server[1] (http://vadar.wishartlab.com/). Residues with φ,ψ angles outside the β sheet region are indicated. The first and last residues of each leader peptide visible in the corresponding crystal structures are highlighted in blue.

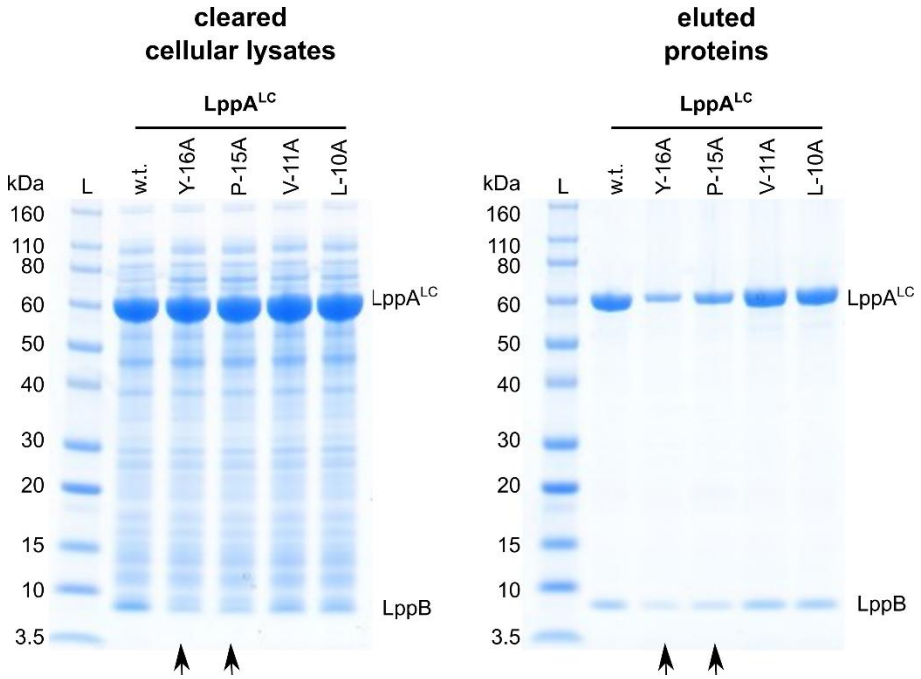

Supplementary Figure 12. Cleared cellular lysates (left) and eluted protein fractions (right) from pull-down assays of LppB in complex with wild-type or mutant $LppA^{LC}$. $LppA^{LC}$ was expressed as an MBP-$LppA^{LC}$-TrxA fusion protein (MW 61.5 kDa). L, molecular weight ladder. Arrows indicate samples in which LppB is largely insoluble in the absence of a bound peptide, resulting in reduced levels in the cleared lysate (left) and consequently decreased recovery of the complex (right). All pull-down experiments were performed independently three times with similar results. Source data are provided as a Source Data file.

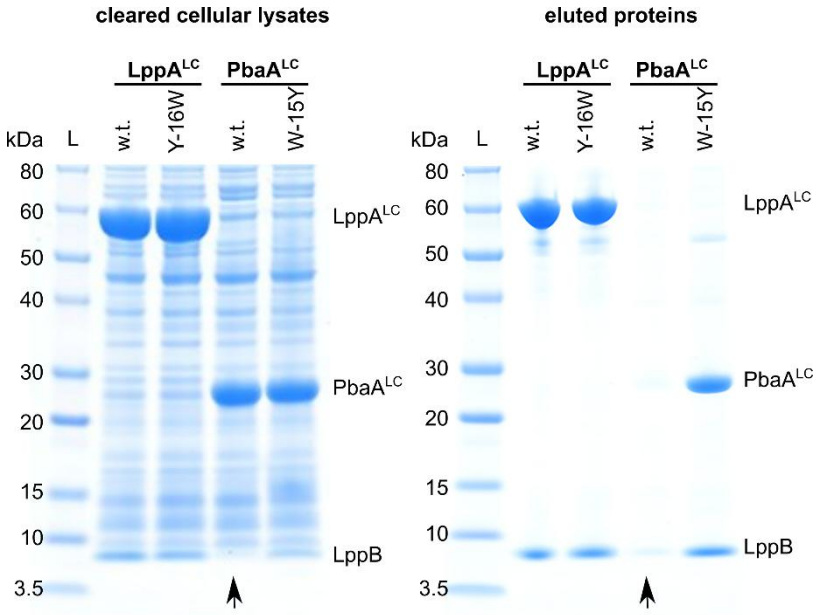

Supplementary Figure 13. Cleared cellular lysates (left) and eluted protein fractions (right) from pull-down assays of LppB in complex with wild-type or mutant LppA^{LC} and PbaA^{LC} peptides. LppA^{LC} was expressed as an MBP–LppA^{LC}–TrxA fusion (MW 61.5 kDa), and PbaA^{LC} as a TrxA–PbaA^{LC}–CBD fusion (MW 24.6 kDa). Arrows indicate samples in which LppB remains predominantly insoluble in the absence of a bound peptide, leading to diminished levels in the cleared lysate and correspondingly lower recovery of the complex. L, molecular weight ladder. All pull-down experiments were performed independently three times with similar results. Source data are provided as a Source Data file.

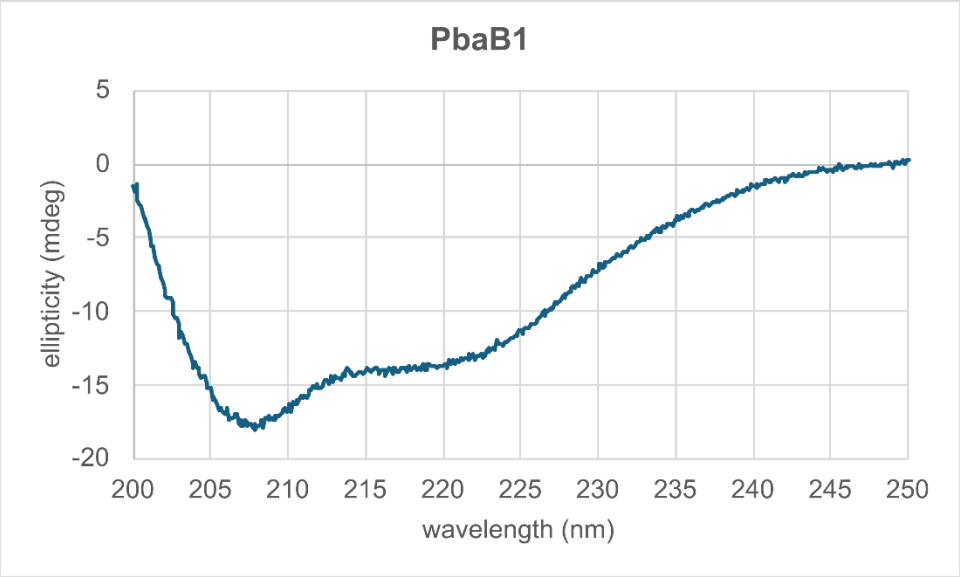

Supplementary Figure 14. Circular dichroism (CD) spectra of PbaB1 recorded at 20 °C. Source data are provided as a Source Data file.

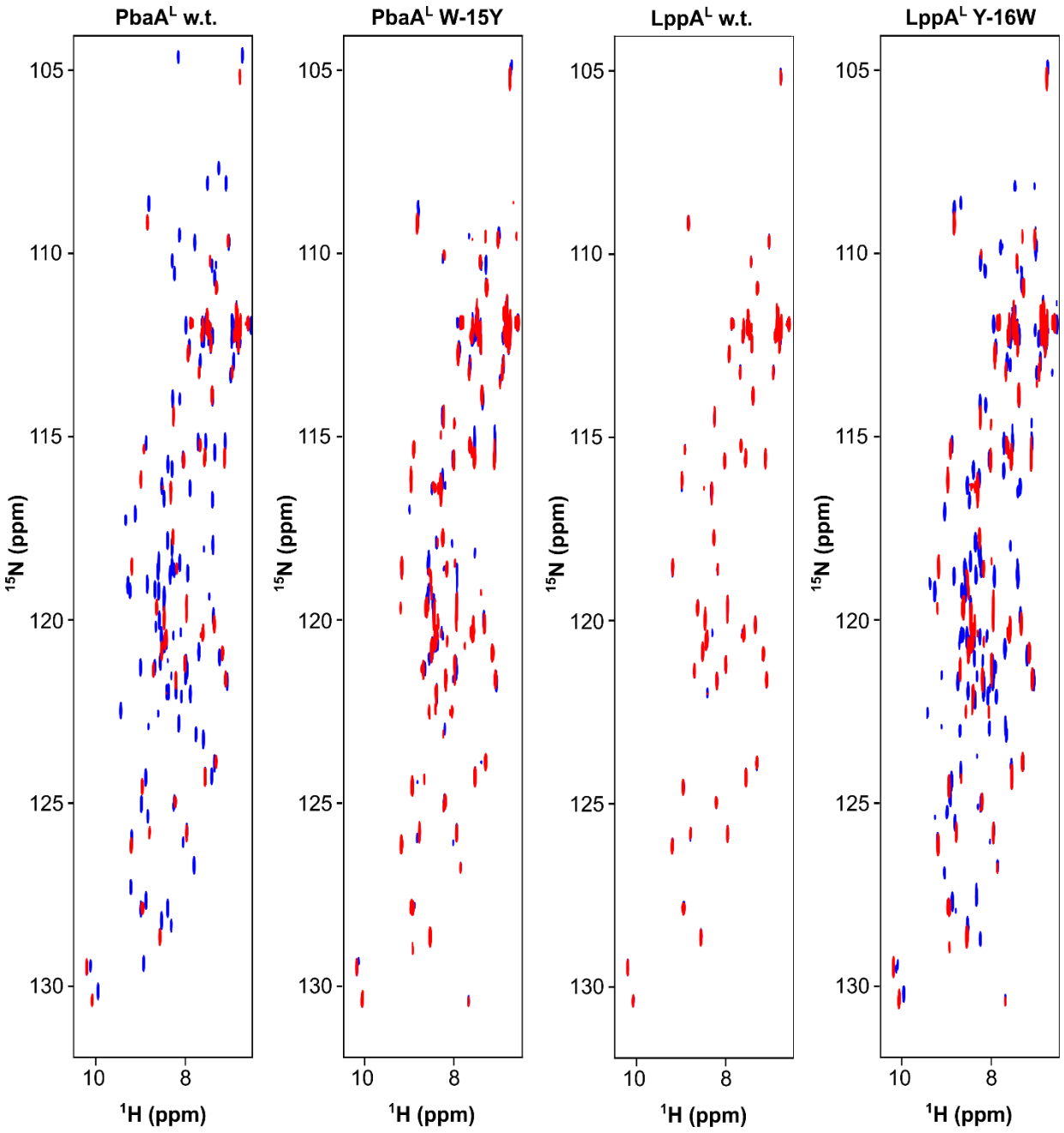

Supplementary Figure 15. ^{1}H, ^{15}N HSQC spectra of the isolated PbaB1 RRE domain (red), and of the same domain in the presence of the indicated peptides in equimolar concentration (blue).

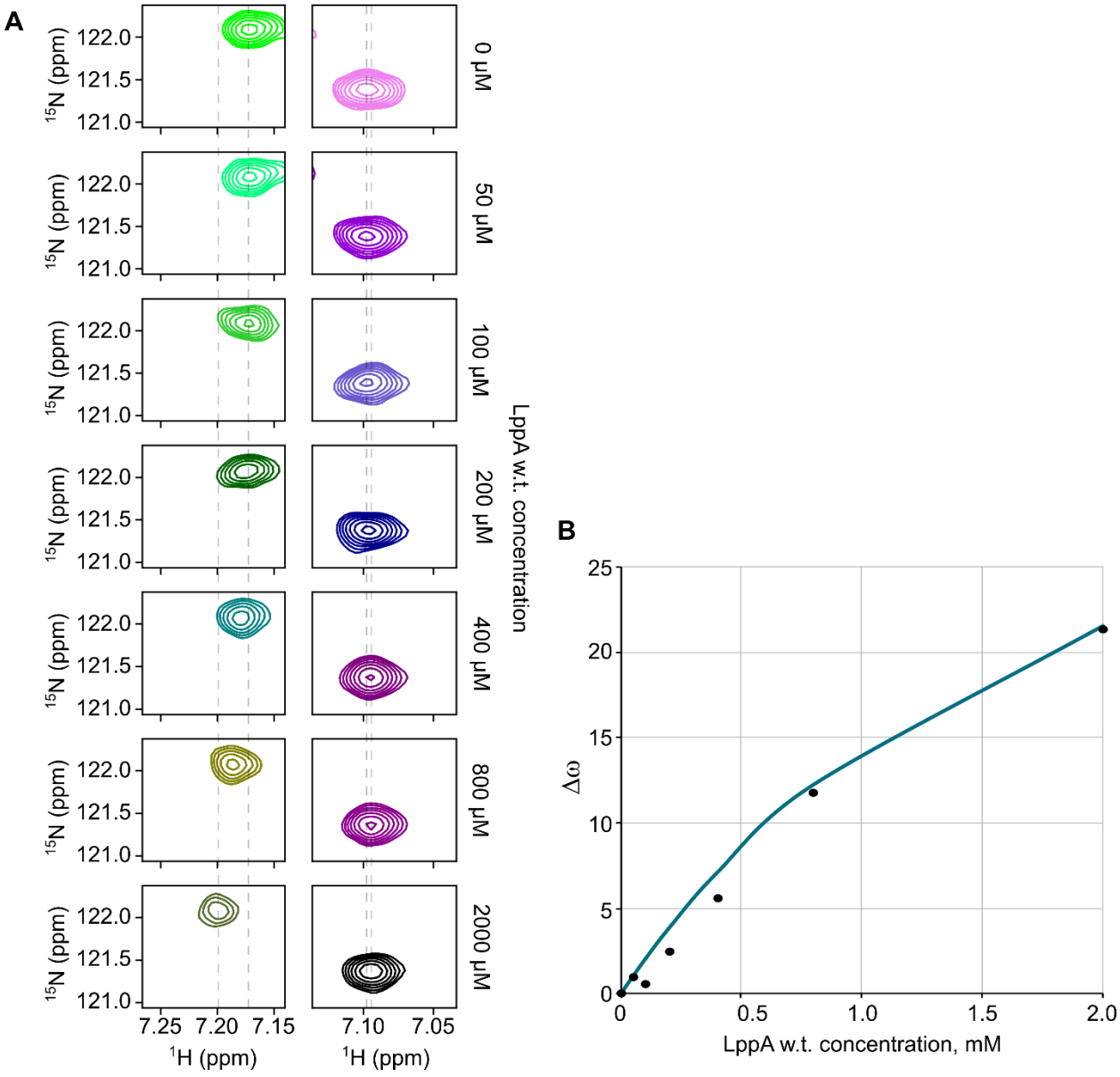

Supplementary Figure 16. (A) ^{1}H,^{15}N HSQC spectra of the PbaB1 RRE domain recorded in the presence of increasing concentrations of the LppA^{L} peptide. **(B)** The chemical shift perturbation of the left resonance was fitted to a 1:1 binding model, yielding a K_D of 1.5 mM. Source data are provided as a Source Data file.

Supplementary Figure 17. Multiple sequence alignment of selected RRE domains from different phyla. Residues corresponding to N33 and D70 in LppB are shown in color. RREs from paeninodin-like lasso peptide BGCs are indicated with an asterisk. The LP column denotes the conserved RRE binding motif of the corresponding peptide precursors.

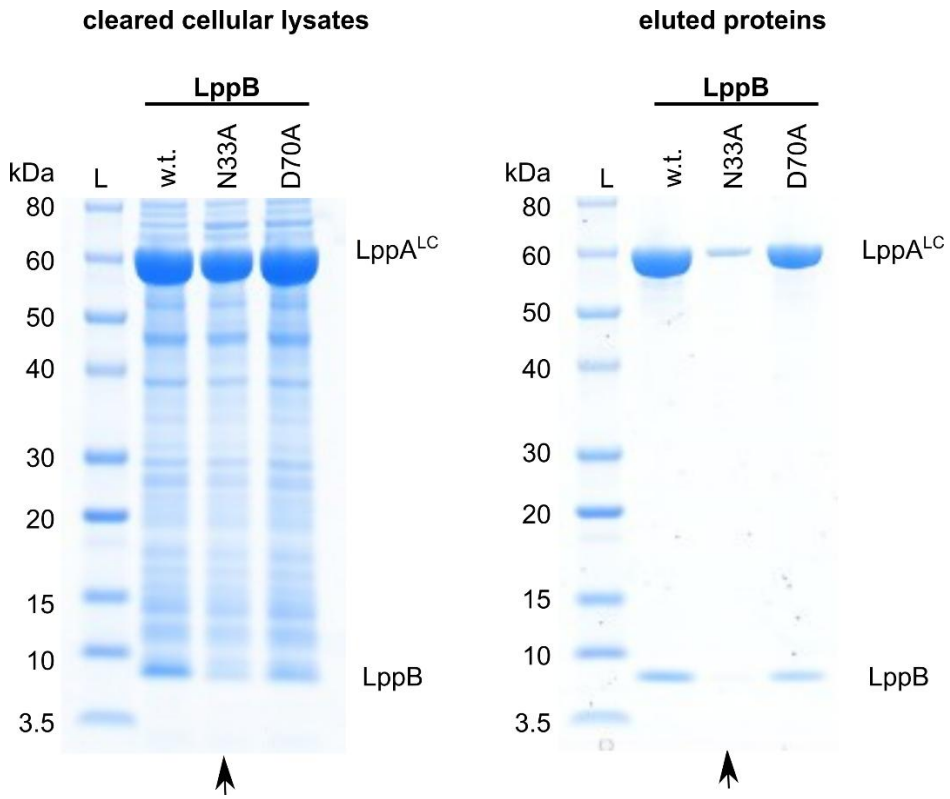

Supplementary Figure 18. Cleared cellular lysates (left) and eluted protein fractions (right) from pull-down assays of wild-type or mutant LppB in complex with the $LppA^{LC}$ peptide. $LppA^{LC}$ was expressed as an MBP–$LppA^{LC}$–TrxA fusion protein (MW 61.5 kDa). Arrows indicate samples in which LppB is largely insoluble in the absence of a bound peptide and therefore reduced in the cleared lysate, resulting in a reduced amount of the recovered complex. L, molecular weight ladder. All pull-down experiments were performed independently three times with similar results. Source data are provided as a Source Data file.

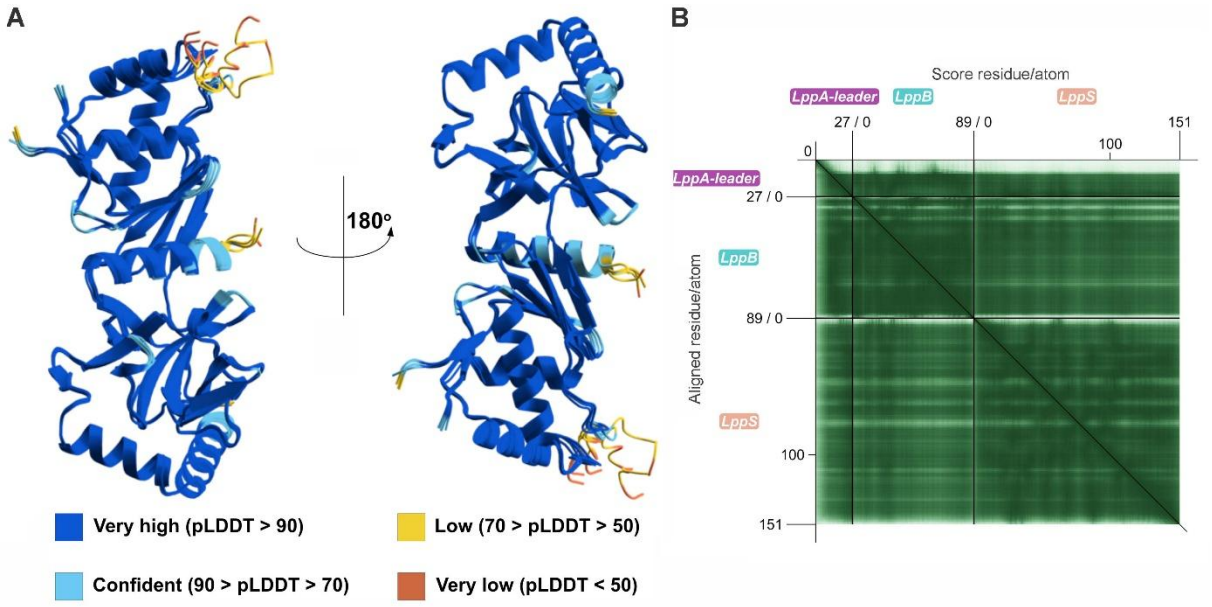

Supplementary Figure 19. AlphaFold3[2] predicted structure of the LppS•LppB•LppA^{L} complex. **A.** Five generated models of the complex overlapped and colored according to the pLDDT score. **B.** Predicted Aligned Error (PAE) plot generated by PAE Viewer[3] online at https://pae-viewer.uni-goettingen.de/.

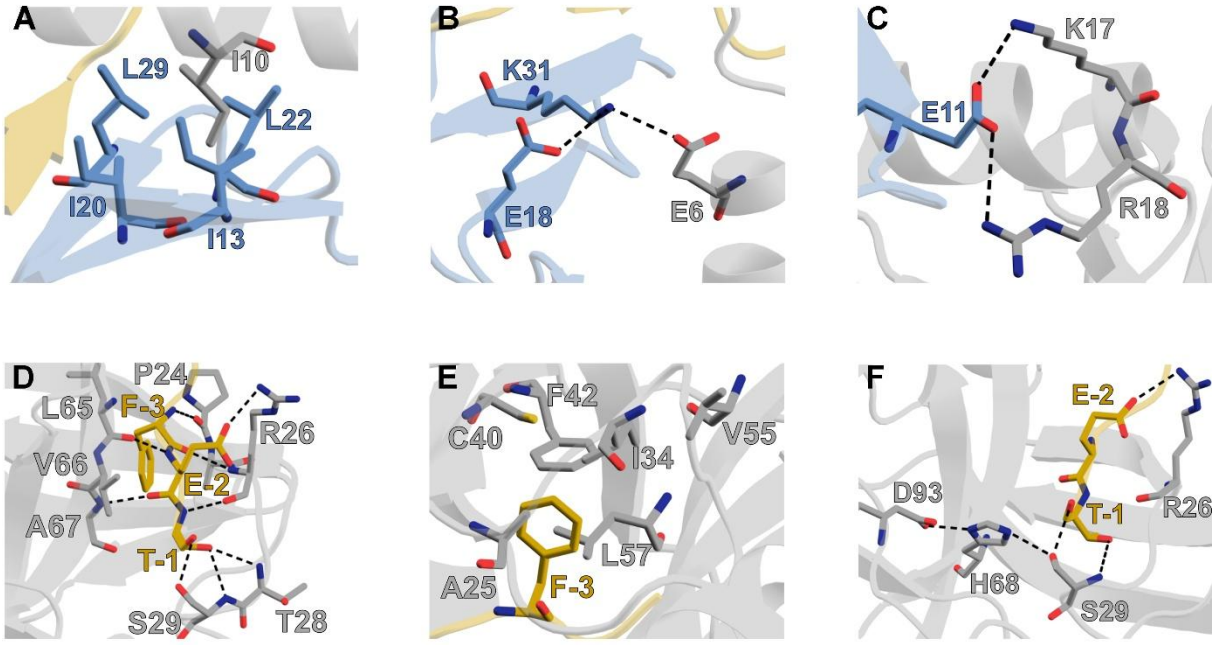

Supplementary Figure 20. Intermolecular interactions in the LppS•LppB•LppA^{L} complex predicted by the AlphaFold3[2] structural model. LppA^{L} is shown in yellow, LppB in blue, and LppS in grey. Hydrogen bonds are indicated with black dashed lines.

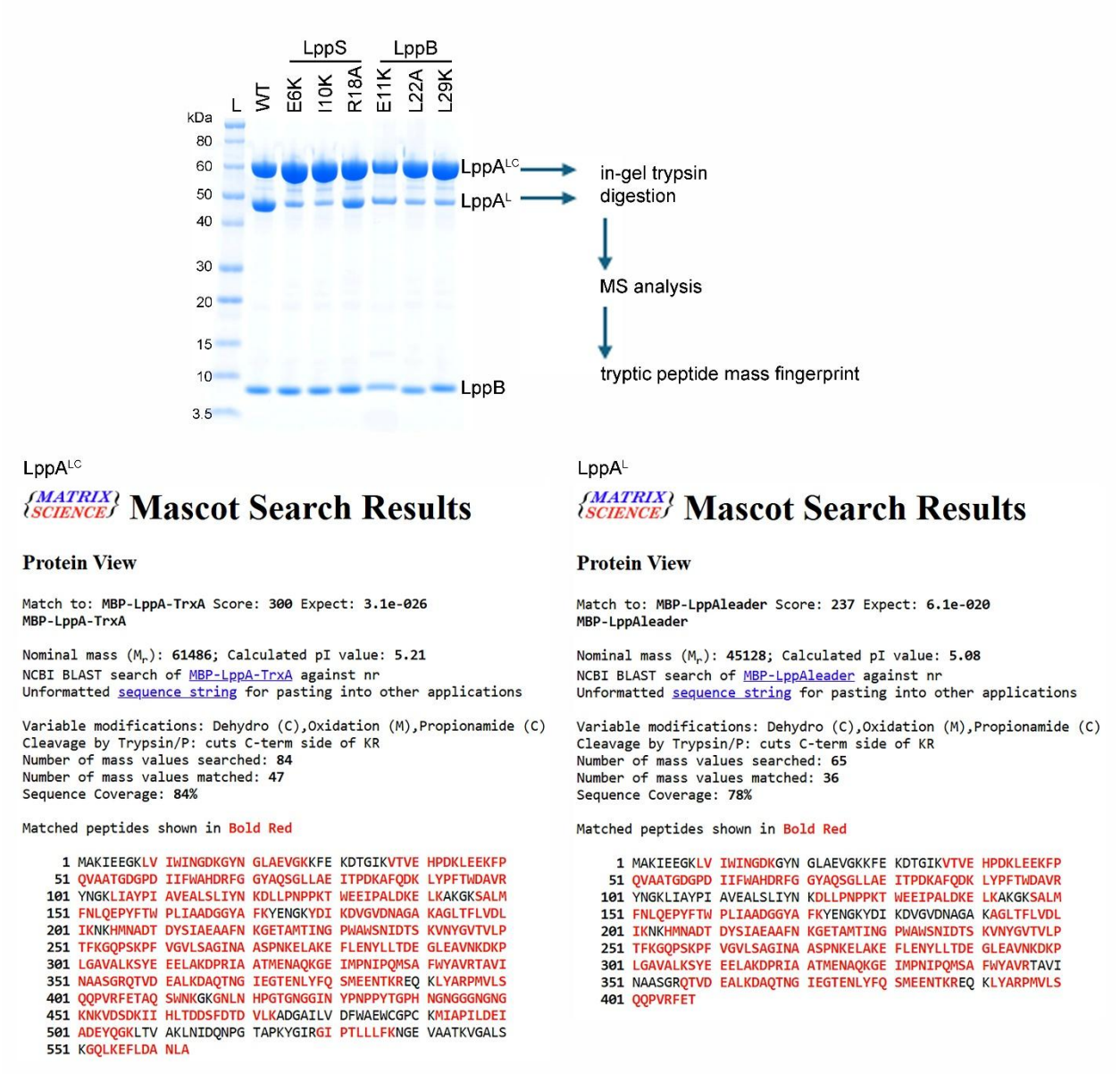

Supplementary Figure 21. Mutational analysis of the LppB–LppS interaction interface in the *in vivo* cleavage/pull-down assay. Mutations in the corresponding proteins are listed at the top. L, protein MW ladder, $LppA^{LC}$, MBP-$LppA^{LC}$-TrxA fusion (MW 61.5 kDa), $LppA^{L}$, $LppA^{L}$ leader peptide fused to MBP (45.1 kDa). Representative tryptic peptide fingerprint analyses confirming correct $LppA^{LC}$ cleavage are shown in the bottom panels. All pull-down experiments were performed independently three times with similar results. Source data are provided as a Source Data file.

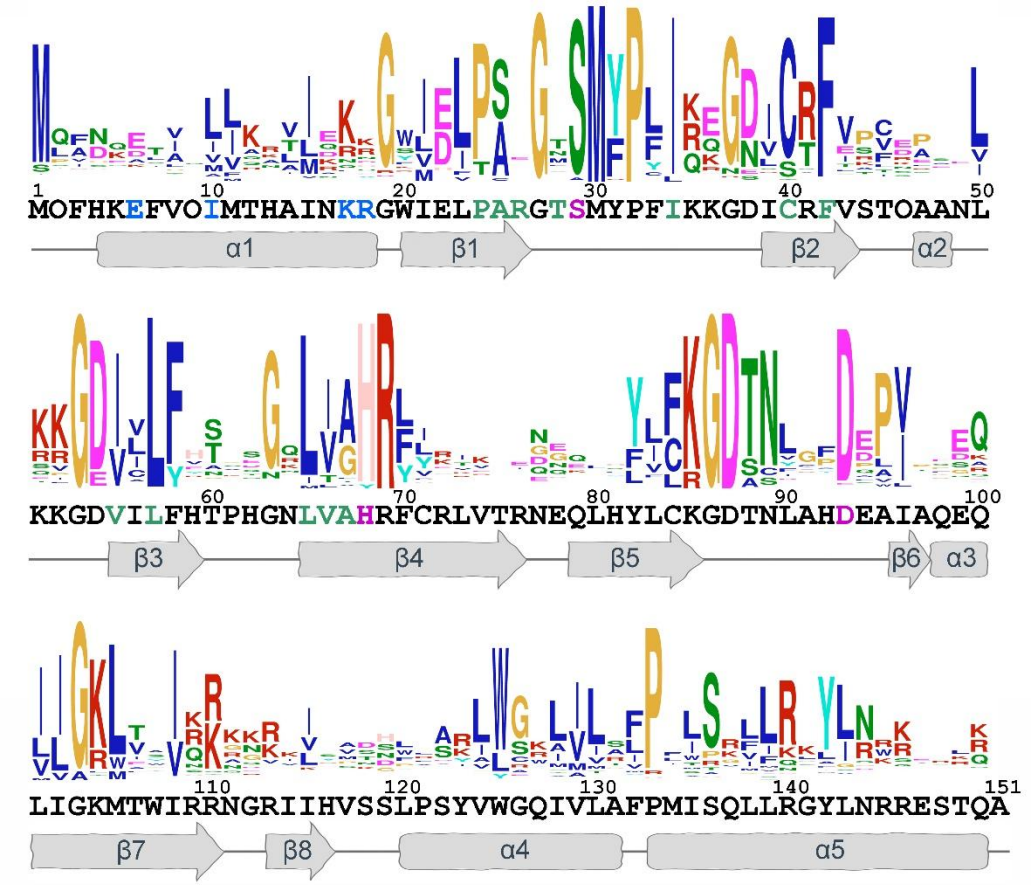

Supplementary Figure 22. The LppS secondary structure and sequence conservation. The conservation of residues is shown as Logo[4]. Secondary structure elements predicted by AlphaFold3 structural model[2] are depicted as arrows (β strands) and rectangles (α helices). Amino acids forming LppS/LppB and LppS/LppA^{LC} intermolecular interfaces are shown in blue and green, respectively. Catalytic residues are in magenta.

A

```
LppK  1    MELFHTQIGEHAIQLICQSEALMC--------------IMRKNFPAADLIVSKPDII---------------IYI---KE  48
BsfK  1    MENTDRLVRYRAFGRDIDGPAGLSlspaPAEAAPGEVPVLRLQ-PDASLRVFIDENLPPLLHNVEDYPGgpKFYVwqEGE  79
PbaK  1    MIEVEKKVVYKAFGLTI-----------VSDVALPELTIVDEQIEEIDIEIKKDEDLTRLYFELTAQPN--QFVV--KDH  65

LppK  49   GYGISFVDYDVEITKEVDSISFRRADYLIEAELDYRYAVISVNN---ELALKHALMNMYSSYVVHHkwGLLIHSSCVMDK  125
BsfK  80   AVGVQYDRWRTRLIPGEGRIDFAELPPS--GPKRVEDAGDEYGRfrfSLAMERVFLPLYALFSMPD--AVALHGSAVVLN  155
PbaK  66   LVIFHIPEIATFSIKEGKRITFSPMKETKDGEIRLLILGTCMG----VILMQRKIFP--------------LHGSLVAIQ  127

LppK  126  GKAYLFAGHSGAGKSTAAKLSMPRN--LLSDEATVVKITSD-KVIIFNSPFRSELDRTT---GAEENSPLAGIYLLNQAV  199
BsfK  156  GEAFLFIGRSGAGKSTTAYEFVRRGATLLADDLIVADVA---RGIALGGAPTLRLWKGE--GALPEAQEDRSLW-RHDAS  229
PbaK  128  GKAYAIIGDSGAGKSTLASAFLNEGYQLLSDDVIAVWLSGEnMPYVTSSYPQQKLWQDSltNFGMESSEYQSLYGRVD--  205

LppK  200  DNHIVPLSKS-----------------------------------------NGFLHLMDKVFYWSH-SPEEIGGILQLL  236
BsfK  230  KRWFRIPAERGAASAVPIAAIVML----DPDTLGGQRDVLPGLET---SPQRKALTDLLGQTFDLSHgTPEWMVARFRNT  302
PbaK  206  -KYYIPVSSKYFTGSLPLAGVIELvkteDKEIAIRQIAKLERFKTlfyHTYRNFLIPDLGLT--------EW---HFNTS  273

LppK  237  QQLVNSVSICELHFQKN--------DTFWELIS-----  261
BsfK  303  ARLIREYPFYHFRYVKSADGKPTHMDALYQAIVGLAsk  340
PbaK  274  VSIVNNVQMFQLSRPASGFTAPQLVTTIMETLNLEA--  309
```

B

```
LppN  1    MI----------------ITLIQALYDpRVPIPQEIEFFDK----------ALEDIEFFDISPQIYWLLKQRGQlVQMPP  54
PbaN  1    ME---NDFRSDSMHFSKELTLLLSIM--RMDKGESMLWKDQDQaneidwGAFLQLARHHRVFSLLYTNLRQTDS-AWIPT  74
BsfN  1    MNapcNEKLASTRLFPEDCPTTSLVLE-RIVEGSALCAGDIAH------ERLLTDADAAGFLPVLYRYLLSTGR------  67

LppN  55   FFQEQLQQKYNGTIYQNMFIRSQTKIALEKLEEAGIQTIPLKGTFFAEKYFGHLGARGTSDIDLLVQPFDLERAIHCVKS  134
PbaN  75   YVMNALQKDYQENTFNMLRLSAEMEQICKLFSESDIRTIVLKGPVLADDLYGNISLRTSRDLDILIPIQHVDQAHELLRS  154
BsfN  68   DVPGRFRQSWLVHIARLALYRAELRRVLPIIEAFS-PVVLLKGEGLSLLLFGDARLRNTTDMDLLIDPRQLGPIVEALGE  146

LppN  135  LGYIEQERIPS--------HFHWSFSKEiPESPIPLTIELHWDLMKEKTSDINMDEFWEQATAIGSYRY---IKELSDYH  203
PbaN  155  QGYVKEEEYNTIlddwKWRHHHATFIH--PDKRV--TLEIHWRLGPGPGKEPGFDELWERKRISKITSH--PVYYLGRED  228
BsfN  147  IGYHTLGDGKTK----PWAYNQLLLVHE----DCGTLIELHWRIAFPHLKSPPIGDLLEDTIAVELDGGalPARSLRPEL  218

LppN  204  TFYMICLHGWRHNLCSLKYFLDIIQMIHILQDKIDYIRLQKDAATHKT---LRRTVRTLAIVYH----------------  264
PbaN  229  LFLFLASHGARHGWSRLRWLIDMDRITRQNIDYAKLHTLLTKNRQLHL---GAQAMILAAQLLHtpLTAEMESMTTGKRA  305
BsfN  219  LLLQLCFHFHQHH-GFYKGLLDIAGWIDRFESTADLDEVRALTRRYEIdgvLQWGLHALERFTG--VRSRLYDPHANLFA  295

LppN  265  ---------HFPHLAGIKELPIKKGINLWWQ------------YNAIRDRNYKTYIQYVNWVYYEF-FDFDSLAHTWAAL  322
PbaN  306  KRLAADALFYIRQMVNLHTAPVPEHVSKYHK------------KHLFSLMSAQQKILFVLSFFYPYpEDADTL--TLPKR  371
BsfN  296  KSWAAWSALEMERRYIFMASP--NAIDRWWRdprvttqiagvlADALSMTVADGALNRLRAVLSPV-----LLGPHRVGR  368

LppN  323  VNFTYS-----IGNMRLSHKIKKM---  341
PbaN  372  LHFLYFPlrpVLWAWRKTNSISQRGT-  397
BsfN  369  VNFAILE---GIGAFGREELYERRILg  392
```

Supplementary Figure 23. Alignments of kinases (A) and NTP transferases (B) from *lpp*, *pba*, and *bsf*[5] BGCs. Identical residues are highlighted in red.

Supplementary Table 1. Data collection and refinement statistics

Name	LppB•LppA^L	PbaB1•PbaA^L
PDB ID	pdb_00009x8z	pdb_00009x90
Data collection		
Beamline	PF BL5-A	SPring8 BL32XU
Wavelength (Å)	1.00	1.00
Space group	P $2_12_12_1$	P 4_3
Unit cell parameters: a; b; c (Å) α; β; γ (°)	 52.90; 55.60; 83.87 90; 90; 90	 49.79; 49.79; 135.01 90; 90; 90
Resolution (Å)	50.00 – 2.10 (2.15 – 2.10)	50.00 – 2.00 (2.05 – 2.00)
$CC_{1/2}$	99.80 (74.40)	99.70 (79.90)
I/σ	11.69 (1.79)	11.12 (2.56)
Completeness (%)	98.20 (97.10)	99.10 (99.80)
Unique reflections	27534* (2023*)	21968 (22169)
R_{meas} (%)	13.50 (104.60)	21.10 (118.50)
Refinement statistics		
Resolution (Å)	32.85 – 2.10	46.71 – 2.00
Reflections	27532*	21957
R_{work}	0.20	0.23
R_{free}	0.25	0.26
Number of atoms (total)	1814	1959
Number of protein atoms	1720	1685
Number of water atoms	94	274
RMSDs		
Bond length (Å)	0.007	0.007
Bond angles (°)	0.943	0.852
Ramachandran plot		
Outliers (%)	0.00	0.00
Allowed (%)	1.95	0.96
Favored (%)	98.05	99.04

Values in parentheses are for the high-resolution shell

*Anomalous data

Supplementary Table 2. Synthetic DNA fragments used in the study

DNA fragment ID	Manufacturer	Sequence
lppA^{LC}-sfGFP	Thermo Fisher	gcgaattaatacgactcactatagggcttaagtataaggaggaaaaaatatgaaaataaaa acaggagcacgcaataacatggaagaaaatacgaagagggaacaaaaattgtatgcgc gccccatggttttaagtcaacaacccgttcgatttgagacagctcaaagctggaataaggg gaaaggtaacctaaatcacccgggtacagggaatggcggcattaattatccgaaccctcc gtacaccggaccgcataatggtaacggaggcggcaacggtaacggtaagaataagcat caccatcatcaccactccgcggctcttgaagtcctctttcagggacccatgagcaaagga gaagaacttttcactggagttgtcccaattcttgttgaattagatggtgatgttaatgggcaca aattttctgtccgtggagagggtgaaggtgatgctacaaacggaaaactcacccttaaattt atttgcactactggaaaactacctgttccatggccaacacttgtcactactctgacctatggt gttcaatgcttttcccgttatccggatcacatgaaacggcatgacttttcaagagtgccatg cccgaaggttatgtacaggaacgcactatatctttcaaagatgacgggacctacaagacg cgtgctgaagtcaagtttgaaggtgataccttgttaatcgtatcgagttaaaaggtattgatt ttaaagaagatggaaacattctcggacacaaactcgagtacaactttaactcacacaatgt atacatcacggcagacaaacaaaagaatggaatcaaagctaacttcaaaattcgccacaa cgttgaagatggttccgttcaactagcagaccattatcaacaaaatactccaattggcgatg gccctgtccttttaccagacaaccattacctgtcgacacaatctgtcctttcgaaagatccca acgaaaagcgtgaccacatggtccttcttgagtttgtaactgctgctgggattacacatggc atggatgagctctacaaaggtagctaataaggaccgaattctgtacaggcc
trxA-pbaA^{LC}	Thermo Fisher	agcgataaaatcatccatctgaccgatgatagctttgataccgatgttctgaaagcagatgg tgcaattctggttgatttttgggcagaatggtgtggtccgtgtaaaatgattgcaccgattctg gatgaaatcgcggatgaatatcagggtaaactgaccgttgcaaaactgaacattgatcag aatccgggtacagcaccgaaatatggtattcgtggtattccgacactgctgctgtttaaaaa cggtgaagttgcagcaaccaaagttggtgcactgagcaaaggtcagctgaaagaatttct ggatgccaatctggcaggcaccgaaaatctgtattttcagagcatgaaaaaagaatggttg aaacctgagcttgaagtattggatgttaatcaaacaatgcttgatccgaaaaatggtaacca ccttgatcatgcttatacggaaggtactcctaaagacaaattaacatggagctaa

Supplementary References

1. Willard, L. *et al*. VADAR: a web server for quantitative evaluation of protein structure quality. *Nucleic Acids Res*. **31**, 3316–9 (2003).
2. Abramson, J. *et al*. Accurate structure prediction of biomolecular interactions with AlphaFold 3. *Nature* **630**, 493–500 (2024).
3. Elfmann, C. & Stülke, J. PAE viewer: a webserver for the interactive visualization of the predicted aligned error for multimer structure predictions and crosslinks. *Nucleic Acids Res*. **51**, W404–W410 (2023).
4. Crooks, G. E., Hon, G., Chandonia, J.-M. & Brenner, S. E. WebLogo: A Sequence Logo Generator. *Genome Res*. **14**, 1188–1190 (2004).
5. Duan, Y. *et al*. Leader peptide removal in lasso peptide biosynthesis based on penultimate isoleucine residue. *Front. Microbiol*. **14**, 1181125 (2023).